

Modeling relaxation and jamming in granular media

B. Kahng^{1,2}, I. Albert¹, P. Schiffer³, and A.-L. Barabási¹

¹ *Department of Physics, University of Notre Dame, Notre Dame, IN 46556*

² *Department of Physics and Center for Advanced Materials and Devices, Konkuk University, Seoul 143-701, Korea*

³ *Department of Physics, Pennsylvania State University, University Park, PA 16802*

(October 31, 2018)

We introduce a stochastic microscopic model to investigate the jamming and reorganization of grains induced by an object moving through a granular medium. The model reproduces the experimentally observed periodic sawtooth fluctuations in the jamming force and predicts the period and the power spectrum in terms of the controllable physical parameters. It also predicts that the avalanche sizes, defined as the number of displaced grains during a single advance of the object, follow a power-law, $P(s) \sim s^{-\tau}$, where the exponent is independent of the physical parameters.

PACS numbers:45.70.Mg, 45.70.Cc, 45.70.Ht

Granular materials are composed of many solid particles that interact only through contact forces, displaying a variety of behavior that distinguishes them from other forms of matter such as liquids or solids. While granular materials can flow like a liquid, unlike liquids, they reach a jammed state when stressed [1]. In the jammed state, which has analogies in a variety of physical systems such as dense colloidal suspensions, traffic flows, and spin glasses [2,3], the local dynamics of grains is frustrated by close contacts between neighboring grains. Although jamming in granular materials has previously been discussed in the context of the gravitational stress induced by the weight of the grains, it can be induced by any compressive stress, such as the stress generated by an object traveling through a granular material. Indeed, there is experimental evidence [4,5] that a solid object being pulled slowly through a granular medium is resisted by local jamming, and can only advance with large-scale reorganizations of the grains. The jamming and reorganization phenomenon, which can be detected through the drag force acting on the object in granular medium, reflects both the nature of stress propagation through the medium and the dynamics of the granular medium [6–15]. The drag force opposing the motion of the object originates in the force needed to induce such reorganizations and exhibits strong fluctuations with a stick-slip character associated with the reorganization of the grains [5]. While these phenomena were documented extensively experimentally, a theoretical microscopic study of the behavior of jamming and relaxation of the drag force has never been attempted.

In this paper we introduce a microscopic model for the motion of a vertical cylinder through a granular medium, describing the jamming and reorganization of grains in terms of compression and relaxation of elastic springs [16] with random thresholds. The model can reproduce many of the experimentally documented features of the drag force, such as the sawtooth shape of the temporal behavior and the main features of the power spectrum. It predicts the period of the sawtooth pattern in terms of physical parameters such as depth, diameter,

and cylinder velocity in agreement with recent experimental results [5,4,17]. In the jammed state, it predicts an avalanche-like relaxation of the grains, the avalanche size following a power-law distribution. The model also predicts that the critical relaxations generating the sudden drops are nucleated preferentially from the bottom part of the cylinder. Finally, we find that the temporal pattern of the drag force can change depending on the elasticity of the grain medium: when grains are rigid the temporal pattern is periodic and the avalanches follow a power-law, however, when they are more elastic, the temporal pattern is random and the avalanche size decays exponentially.

Microscopic model — The model was constructed to emulate the drag experienced by a vertical cylinder of diameter d inserted to a depth H in a granular bed [4,5]. The grains move with constant speed v in the positive x direction, pushing the cylinder in the same direction. The motion of the cylinder is constrained by a fixed stop which is coupled to the cylinder through an external spring with spring constant K . The force on the fixed stop is equivalent to the drag force, $F(t)$, on the cylinder as a function of time. We refer to the spring located between the cylinder and fixed stop as the external spring. As the granular medium moves in the positive x direction, the grains in contact with the cylinder’s surface push the cylinder with small forces whose sum is the total drag force. To model the heterogeneous nature of granular drag we regard the surface of the cylinder as a planar rectangle partitioned into $d \times H$ cells of unit size.

Grains push the cylinder only if they are compressed, and we thus model each cell as a ”grain-spring”. The magnitude of the force $f_{i,j}(t)$ exercised by the spring in cell (i,j) ($i = 1..d$, $j = 1..H$) is given by Hooke’s law, $f_{i,j} = f_{i,j}(0) + k_{i,j}x_{i,j}$ where $f_{i,j}(0)$ is the x component of the ambient force, $k_{i,j}$ is the grain spring constant, and $x_{i,j}$ is the deviation of the spring’s length from its uncompressed value. It is well known that the pressure in granular media increases linearly with depth and will increase the ambient force $f_{i,j}(0) = f_{0j}$ [19]. The grain-spring constant should be interpreted as describing

the elasticity of the force chains instead of the individual grains. The force chains are expected to get stiffer with depth, since the participating grains are more compressed, allowing less room for configurational changes. Thus we expect that the spring constant $k_{i,j}$ will also increase linearly, $k_{i,j} = k_0 j$.

If the grains are too compressed, they will fail by slipping relative to the cylinder's surface and each other, thus relaxing the local forces. As a result, the total force acting on the cylinder decreases, and the cylinder slips relative to the grains. To model this microscopic failure we introduce a critical threshold $g_{i,j}$, which is a random variable uniformly distributed between $[g_0 j, g_1 j]$, where g_0 and g_1 are constants. When the elastic force on a grain spring exceeds its critical threshold, ($f_{i,j} \geq g_{i,j}$), the spring is relaxed to its equilibrium position, $f_{i,j} = f_{i,j}(0)$, and the threshold $g_{i,j}$ is newly updated by a new random number.

As grains advance in the positive x -direction by the distance $v\delta t$ during time interval δt , they increase the total force acting on the cylinder, compressing the external spring K as well. The balance between the cumulative action of the grain springs and the opposing force of the external spring allows the cylinder to move in the $+x$ direction by a distance ℓ ,

$$\ell = k_t v \delta t / (k_t + K), \quad (1)$$

where $k_t = k_0 dH(H + 1)/2$, is the collective spring constant of the grain springs. The distance (1) was obtained by balancing the collective elastic forces of the grain springs and the external spring on each side of the cylinder,

$$\sum_{i,j} k_{i,j} \delta x_{i,j} = K\ell, \quad (2)$$

where $\delta x_{i,j} = v\delta t - \ell$. After obtaining ℓ , the effective compression of grain springs can be determined from $\delta x_{i,j} = K v \delta t / (k_t + K)$, leading to an increase in the grain spring force by $\delta f_{i,j} = k_0 j K v \delta t / (k_t + K)$. When the grain springs are much stiffer than the external springs ($k_t \gg K$), corresponding to the case in which the experiment was performed, the increased grain spring force acting on the cylinder at (i, j) becomes

$$\delta f_{i,j} = k_0 j K v \delta t / k_t. \quad (3)$$

The situation suddenly changes if a grain slips, i.e. the force $f_{i,j}$ on a grain spring reaches its threshold $g_{i,j}$. We reset the force to $f_{i,j}(0)$, and the threshold is updated [18]. After this update, the balance between the elastic forces on each side of the cylinder breaks down, because the total force acting from the grains on the cylinder has dropped by $f_{i,j}(t) - f_{i,j}(0)$. As a result the cylinder will move backward (in the negative x direction), pushed by the external spring, compressing further the remaining grain springs. The displacement of the cylinder can be calculated by using the balance equation (2), where the

newly updated sites (i.e., those having $f_{i,j} = f_{i,j}(0)$) are excluded from the summation.

There are two possible outcomes of this slip event. First, if this sudden compression of all grain springs will not cause any more springs to reach their thresholds, after establishing a new equilibrium we continue the continuous compression of all springs by the motion of the grains with velocity v . However, in some cases the discontinuous increase of the force on the grain springs will cause some other springs to reach their thresholds. In this case the updating (replacing each broken spring with an uncompressed one and calculating the new equilibrium) is repeated until no further reorganizations occur. The time is then incremented, followed by the advance of all grain springs, leading to a repetition of the above processes through compression and new updating. The dynamics of the model are similar to the random fuse model in one dimension [20] describing fracture of a fiber bundle in the sense that when one spring (bond) breaks down, the load from it is shared by others. There is a significant difference, however, in that within the current model the springs can be re-compressed, resulting in a stationary dynamics, while in the random fuse model a bond is permanently disconnected once it has burned out.

The stochastic model described above offers a microscopic description of the system investigated experimentally. Despite its simplicity, as we show next, it accounts for many key factors of the observed behavior, and offers insight and quantitative predictions that were not available experimentally [4,5].

Sawtooth pattern — A characteristic feature of the drag force observed in the experiments is that the force on a cylinder, $F(t)$, increases linearly, followed by a sudden drop in $F(t)$, corresponding to a collective failure and reorganization of the grains. As Fig. 2a-c shows, this sawtooth pattern is fully reproduced by the model. The linear increase corresponds to a continuous compression of both the grain springs and the external spring. At a certain point, however, a grain spring fails, which results in a collective and subsequent failure of all other springs in the system, since they are compressed to near their thresholds. Thus the stick-slip motion observed in the experiments correspond to two regimes: in the linear regime we see a linear convergence to the critical state, where all the springs are more or less simultaneously compressed towards their critical threshold. The sudden drop corresponds to an avalanche like spreading of a failure as soon as the critical or fragile state has been reached. The advantage of the presented model is that it allows us to quantitatively characterize the resulting stick-slip process.

Linear Regime — What does determine the slope of the $F(t)$ signal in the linear regime? Eq. (4) predicts that the drag force, $F(t) = \sum_{i,j} f_{i,j}(t)$, increases linearly with time with the slope $\frac{1}{v} \frac{dF}{dt} \sim K$ in the jammed state. This linear increase is in complete agreement with the experimental results (see Fig. 2 of [5]). Furthermore we

predict that the slope is independent of the experimental details, but depends only on the spring constant of the external spring, which is again consistent with the experimental findings.

Failure and depth dependence — When updating occurs over the entire system, the drag force drops suddenly, because most grain springs are reset to their equilibrium positions, and $f_{i,j}(t) = f_{i,j}(0)$. Accordingly, we expect the drag force to exhibit a sawtooth pattern. This is supported by extensive numerical simulations whose results are summarized in Fig.2a-c. This allows us to determine the average value of the drag force, that has been investigated extensively both experimentally and numerically (see Ref. [5]). Since the force at (i, j) is independent of i and proportional to j , we find that the average drag force \bar{F} over time is proportional to $\sim dH^2$. This result is confirmed by numerical simulation as well (see Fig.2d), and is in agreement with the experimental results [5].

Power spectrum — To better characterize the fluctuations in the system, we measured the power spectrum of the time dependent drag force as predicted by the model. In [5] it has been found that the power spectrum is characterized by a few prominent peaks and sub-harmonics, determining the period of the signal, followed by a power-law tail at high frequencies which decays as f^{-2} . The numerically determined power spectrum has the same features (Fig 2e), exhibiting an $\sim 1/f^2$ behavior at high frequencies and peaks at low frequencies. The origin of the $1/f^2$ behavior comes from fluctuations of critical relaxation time due to random thresholds. The position of the largest peak corresponds to the inverse of the period of the sawtooth pattern. Thus, estimating the peak position, we can determine $(1/T)$, the period of the sawtooth signal (see the inset of Fig.2e). Furthermore, this period can be predicted analytically as follows: the critical updating occurs when $\delta f_{i,j}$ is increased to the maximum value of threshold $\sim jg_1$. The time required to reach this critical force through jamming is

$$T \sim k_t(g_1 - g_0)/(k_0Kv) \sim (g_1 - g_0)H^2d/Kv, \quad (4)$$

which represents the period. The numerical simulation data for different depths, diameters, and elastic spring constants K (shown in the inset of Fig.2e) confirm Eq.(4), and are also in agreement with recent experimental results [17].

Avalanches — A quantity that has not been measured experimentally, but can be determined in the present model, is the avalanche size distribution $P(s)$. When a collective failure occurs, this will result in the simultaneous failure of a certain number of grains springs (but not all) creating an avalanche of failures. The avalanche size, s , is defined as the number of springs newly updated in a single advance of the cylinder. We find that the avalanche size follows a power-law distribution, $P(s) \sim s^{-\tau}$ with $\tau \approx 2.4(1)$ (see Fig. 3a). Since power-law distribution of events are common only at the critical point of spatially extended systems indicating that the continuous compression of the grains brings the system close to a critical

state. Furthermore we find that the exponent τ is universal, independent of physical parameters such as depth H , width d , spring constant K , grain spring constant k_0 , and threshold $g_1 - g_0$. Note that while the avalanche sizes could not be measured experimentally, bulk imaging techniques such as MRI, allowing one to compare the grain positions before and after an avalanche, could offer a quantitative check of our predictions.

The simulations indicate that the critical avalanches are nucleated preferentially near the bottom of the cylinder where the stress is largest (see inset to Fig. 3a). When a spring at large H is relaxed suddenly, the load taken over by the other springs is commensurately large, and has a higher probability of nucleating a large-scale reorganization of the grains. In contrast, breakdown of springs at small H is less likely to nucleate avalanches.

Finally, the model predicts that the elastic properties of the granular media have a strong impact on the temporal characteristics of the drag force. When grains are sufficiently soft, $k_t \ll K$, the drag force develops a random signal rather than sawtooth, (inset to Fig. 3b). Such random characteristics also occur when the depth H is small enough to satisfy the condition $k_t \ll K$ for a given grain spring constant k_0 . Interestingly, in this case, the avalanche size distribution does not follow a power-law, but decays exponentially as shown in Fig. 3b.

In summary, we have introduced a stochastic model that describes the jamming and reorganization of grains associated with dragging an object through a granular medium. The model reproduces the sawtooth pattern of temporal evolution of the drag force and the $1/f^2$ high frequency tail of the power spectrum, and predicts a power-law avalanche size distribution. This excellent agreement with the experiments is surprising because the model offers a mean-field treatment of the force chains which are known to be the basic mechanism of the stress propagation through grains. Indeed, the force chains are only included implicitly through the depth dependence of the grain-spring elastic constant. Thus improvements based on a more detailed handling of the force chains could be envisioned, but our model offers a crucial starting point for a detailed understanding of motion through granular media, and it offers a basis for more realistic modeling efforts.

This work is supported by the Petroleum Research Fund administered by the ACS, the Alfred P. Sloan Foundation, NSF Grants No. PHYS95-31383 and No. DMR97-01998, NASA grant number NAG3-2384 and by grants No. 2000-2-11200-002-3 from the BRP program of the KOSEF.

[1] M.E. Cates, J.P. Wittmer, J.-P. Bouchaud, and P. Claudin, Phys. Rev. Lett. **81**, 1841 (1998); M.E. Cates

- and J.P. Wittmer, *Physica (Amsterdam)* **263A**, 354 (1999).
- [2] A.J. Liu and S.R. Nagel, *Nature (London)* **396**, 21 (1998).
- [3] C.S. O'Hern, S.A. Langer, A.J. Liu, S.R. Nagel, *cond-mat/0005035*.
- [4] R. Albert, M.A. Pfeifer, A.-L. Barabasi, and P. Schiffer, *Phys. Rev. Lett.* **82**, 205 (1999).
- [5] I. Albert, P. Tegzes, B. Kahng, R. Albert, J.G. Sample, M. Pfeifer, A.-L. Barabasi, T. Vicsek, and P. Schiffer, *Phys. Rev. Lett.* **84**, 5122 (2000).
- [6] H.M. Jaeger, S.R. Nagel, and R.P. Behringer, *Rev. Mod. Phys.* **68**, 1259 (1996); L.P. Kadanoff, *Rev. Mod. Phys.* **71**, 435 (1999).
- [7] C. Liu et al., *Science* **269**, 513 (1995); D.M. Mueth, H.M. Jaeger, and S.R. Nagel, *Phys. Rev. E* **57**, 3164 (1998).
- [8] B. Miller, C. O'Hern, and R.P. Behringer, *Phys. Rev. Lett.* **77**, 3110 (1996).
- [9] X. Jia, C. Caroli, and B. Velicky, *Phys. Rev. Lett.* **82**, 1863 (1999).
- [10] E. Kolb, T. Mazozi, E. Clement, and J. Duran, *Eur. Phys. J. B.* **8**, 483 (1999).
- [11] S.N. Coppersmith et al., *Phys. Rev. E*, 53, 4673 (1996); M.L. Nguyen and S.N. Coppersmith, *Phys. Rev. E* **59**, 5870 (1999).
- [12] A.V. Tkachenko and T.A. Witten, *Phys. Rev. E* **60**, 687 (1999).
- [13] A. Ngadi and J. Rajchenbach, *Phys. Rev. Lett.* **80**, 273 (1998).
- [14] L. Vanel et al., *Phys. Rev. E* **60**, 5040 (1999); D. Howell, R.P. Behringer, and C. Veje, *Phys. Rev. Lett.* **82**, 5241 (1999).
- [15] A.L. Demirel and S. Granick, *Phys. Rev. Lett.* **77**, 4330 (1996); H.J.S. Feder and J. Feder, *Phys. Rev. Lett.* **66**, 2669 (1991).
- [16] M.L. Nguyen and S.N. Coppersmith, *cond-mat/0005023*.
- [17] I. Albert et al. (unpublished).
- [18] Note that we choose $g_0 > f_0$ so that the initial stress f_{0j} is always smaller than threshold, g_{0j} .
- [19] Note that the depth we consider here is shallower than the Janssen's critical depth, thus the average pressure increases linearly for all considered depths.
- [20] B. Kahng, G.G. Batrouni, S. Redner, H.J. Herrmann, L. de Arcangelis, *Phys. Rev. B* **37**, 7625 (1988); B. Kahng, *J. Phys. A* **23**, L49 (1990).

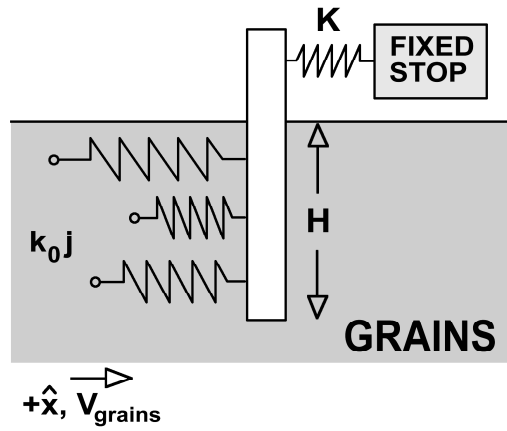


FIG. 1. Schematic illustration of the stochastic spring model. The shaded area indicates the granular medium, which moves with velocity v in the positive x direction. The motion of the cylinder that tries to move along with the grains is opposed by a fixed stop coupled to the cylinder through a spring with spring constant K . We model the grains opposing the movement as springs with spring constant k_{0j} .

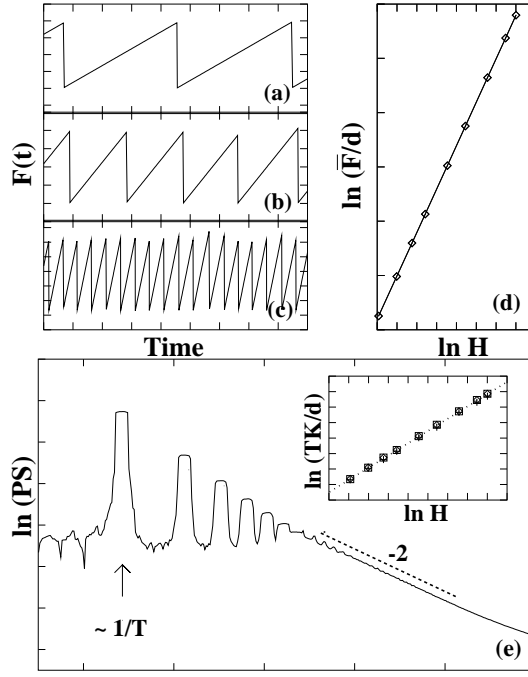


FIG. 2. (a-c) Plot of the drag force $F(t)$ as a function of time for $d = 2, H = 1000$ (a), $d = 1, H = 1000$ (b), and $d = 1, H = 500$ (c), where $f_0 = 0.5, g_0 = 0.5, g_1 = 0.7, K = 1, k_0 = 1$, and $v = 1$ are used. (d) Double logarithmic plot of \bar{F}/d versus H for different diameters $d = 1$ and 5 . The solid line with slope 2.0 is obtained by a least square fit. (e) Double logarithmic plot of the power spectrum (PS) versus frequency. Inset: Double logarithmic plot of TK/d versus depth H for different spring constants $K = 1$ and $K = 5$ and cylinder diameters $d = 1$ and $d = 5$ of the cylinder. The data are well collapsed on the dotted line with slope 1.98 , obtained by a least square fit, predicted by Eq.(4).

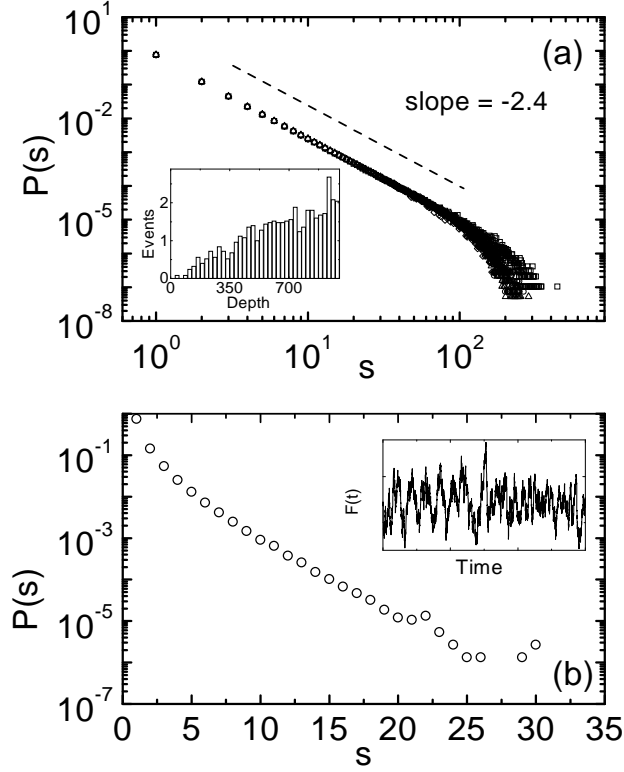


FIG. 3. a) Logarithmic plot of the avalanche size distribution $P(s)$ versus size s for different diameters $d = 1$ and 2 , depths $H = 1000$ and 2000 , elastic spring constants $K = 1$ and 10 , and grain spring constants $k_0 = 1$ and 10 , where critical avalanches which contribute an isolated point are excluded in the accumulation. All data, averaged over 5000 configurations, are collapsed to $P(s) \sim s^{-2.4}$. The inset shows the number of avalanches nucleated at a certain depth averaged over a 25 point depth interval. b) Semi-logarithmic plot of the avalanche size distribution versus size for $k_0 = 10^{-6}$ showing an exponential distribution. The data are averaged over 5000 runs. The inset shows a plot of the drag force as a function of time under the same condition used in Fig.2b, but $k_0 = 10^{-6}$.